

**“Edge-selectively functionalized graphene-like platelets as a co-curing agent and a nanoscale additive to epoxy resin”**

**August 12, 2012**

**Name of Principal Investigators (PI and Co-PIs):**

- e-mail address : jbbaek@unist.ac.kr
- Institution : **Ulsan National Institute of Science and Technology (UNIST)**
- Mailing Address : **100 Banyeon, Ulsan, 689-798 South Korea**
- Phone : **82-52-217-2510**
- Fax : **82-52-217-2019**

Period of Performance: 04/01/2011 – 05/31/2012

**Abstract:** A newly developed method for the edge-selective functionalization of “pristine” graphite with 4-aminobenzoic acid was applied for the synthesis of 4-aminobenzoyl-functionalized graphite (AB-graphite) through a “direct” Friedel–Crafts acylation in a polyphosphoric acid (PPA)/phosphorous pentoxide medium ( $P_2O_5$ ). The AB moiety at the edge of the AB-graphite played the role of a molecular wedge to exfoliate the AB-graphite into individual graphene and graphene-like platelets upon dispersion in polar solvents. These were used as a co-curing agent and a nanoscale additive to epoxy resin. The physical properties of the resulting epoxy/AB-graphite composites were improved because of the efficient load transfer between the additive and epoxy matrix through covalent links.

**Introduction:** Epoxy or polyepoxide resins are widely used commodity thermosetting resins that form via the reaction between an epoxide resin and a polyamine hardener.<sup>1</sup> Epoxy resins have a wide range of applications, including in fiber-reinforced composites,<sup>2</sup> as general-purpose adhesives<sup>3</sup> and in coatings.<sup>4</sup> In general, epoxy resins are known for their excellent adhesion, chemical and heat resistance, good-to-excellent mechanical properties, and their very good electrical insulating properties.

Graphene is currently the focal point for research into condensed matter because of the interesting properties of graphene.<sup>5</sup> Graphene nanoplatelets have exceptional mechanical strength ( $\approx 1,100$  GPa),<sup>6</sup> thermal conductivity ( $\approx 5,000$  W m<sup>-1</sup> K<sup>-1</sup>),<sup>7</sup> specific surface area ( $\approx 2630$  m<sup>2</sup>g<sup>-1</sup> (calc.))<sup>8</sup> and ultra high electron transport properties (200,000 cm<sup>2</sup> V<sup>-1</sup>s<sup>-1</sup>).<sup>9</sup> Graphene is a very attractive material for potential applications in composites,<sup>10,11</sup> energy-related systems,<sup>12</sup> sensors,<sup>13</sup> electronics,<sup>14</sup> photonics,<sup>15</sup> and spintronics.<sup>16</sup> There are two major approaches used in the preparation of graphene. The first method is the exfoliation of “pristine” graphite into graphene, which involves physical<sup>17</sup> and chemical methods.<sup>11</sup> The second method is where graphene can be grown using chemical vapor deposition (CVD) on a metal substrate<sup>18–20</sup> or from single crystal silicon carbide.<sup>21</sup> For mass production, the

Report Documentation Page			Form Approved OMB No. 0704-0188	
<p>Public reporting burden for the collection of information is estimated to average 1 hour per response, including the time for reviewing instructions, searching existing data sources, gathering and maintaining the data needed, and completing and reviewing the collection of information. Send comments regarding this burden estimate or any other aspect of this collection of information, including suggestions for reducing this burden, to Washington Headquarters Services, Directorate for Information Operations and Reports, 1215 Jefferson Davis Highway, Suite 1204, Arlington VA 22202-4302. Respondents should be aware that notwithstanding any other provision of law, no person shall be subject to a penalty for failing to comply with a collection of information if it does not display a currently valid OMB control number.</p>				
1. REPORT DATE <b>27 SEP 2012</b>	2. REPORT TYPE <b>Final</b>	3. DATES COVERED <b>01-04-2011 to 31-05-2012</b>		
4. TITLE AND SUBTITLE <b>Edge-selectively functionalized graphene-like platelets as a co-curing agent and a nanoscale additive to epoxy resin</b>			5a. CONTRACT NUMBER <b>FA23861114042</b>	
			5b. GRANT NUMBER	
			5c. PROGRAM ELEMENT NUMBER	
6. AUTHOR(S) <b>Jong-Beom Baek</b>			5d. PROJECT NUMBER	
			5e. TASK NUMBER	
			5f. WORK UNIT NUMBER	
7. PERFORMING ORGANIZATION NAME(S) AND ADDRESS(ES) <b>Ulsan National Institute of Science and Technology, 100 Banyeon, Ulsan 689-897, Korea (South), KR, 689897</b>			8. PERFORMING ORGANIZATION REPORT NUMBER <b>N/A</b>	
			10. SPONSOR/MONITOR'S ACRONYM(S) <b>AOARD</b>	
9. SPONSORING/MONITORING AGENCY NAME(S) AND ADDRESS(ES) <b>AOARD, UNIT 45002, APO, AP, 96338-5002</b>			11. SPONSOR/MONITOR'S REPORT NUMBER(S) <b>AOARD-114042</b>	
			12. DISTRIBUTION/AVAILABILITY STATEMENT <b>Approved for public release; distribution unlimited</b>	
13. SUPPLEMENTARY NOTES				
14. ABSTRACT <b>A newly developed method for the edge-selective functionalization of ?pristine? graphite with 4-aminobenzoic acid was applied for the synthesis of 4-aminobenzoyl-functionalized graphite (AB-graphite) through a ?direct? Friedel?Crafts acylation in a polyphosphoric acid (PPA)/phosphorous pentoxide medium (P2O5). The AB moiety at the edge of the AB-graphite played the role of a molecular wedge to exfoliate the AB-graphite into individual graphene and graphene-like platelets upon dispersion in polar solvents. These were used as a co-curing agent and a nanoscale additive to epoxy resin. The physical properties of the resulting epoxy/AB-graphite composites were improved because of the efficient load transfer between the additive and epoxy matrix through covalent links.</b>				
15. SUBJECT TERMS <b>composites</b>				
16. SECURITY CLASSIFICATION OF:			17. LIMITATION OF ABSTRACT <b>Same as Report (SAR)</b>	18. NUMBER OF PAGES <b>15</b>
a. REPORT <b>unclassified</b>	b. ABSTRACT <b>unclassified</b>	c. THIS PAGE <b>unclassified</b>	19a. NAME OF RESPONSIBLE PERSON	

efficient exfoliation of “pristine” graphite into individual graphene and/or graphene-like platelets is an important challenge that needs to be overcome.

Hybridization of widely used resins, and newly developed nanomaterials are expected to have novel properties. Until now, research into polymer-based composites has been devoted to achieving the maximum enhancement in properties by adding nanoscale additives. To benefit from the change in properties resulting from nanoscale phenomena, these additives must be uniformly dispersed into, and strongly interacted with, the supporting matrix.<sup>22,23</sup> Thus, ultrasonication,<sup>24</sup> high-shear mixing,<sup>25</sup> use of surfactants,<sup>26</sup> mechanical alignment,<sup>27</sup> chemical modification,<sup>28</sup> and polymer chain wrapping<sup>29</sup> have been applied for both the efficient dispersion and interfacial interaction in the matrix. Among these methods, chemical modification of the nanoscale additives can provide chemical affinity for both purposes, in addition to a variety of functionalities.<sup>30–32</sup> Specifically, the introduction of amine groups onto the surface of an additive can mean using them as hardeners for the epoxy resin.<sup>33</sup>

In this work, the edges of “pristine” graphite were selectively functionalized with 4-aminobenzoic acid to produce 4-aminobenzoyl-functionalized graphite (AB-graphite) using a “direct” Friedel–Crafts acylation in polyphosphoric acid (PPA)/phosphorous pentoxide (P<sub>2</sub>O<sub>5</sub>) medium.<sup>34,35</sup> As a simple and scalable approach, AB-graphite was exfoliated into individual graphene and graphene-like platelets, fulfilling the expectation that the AB-moiety played the role of a “molecular wedge”. Indeed, the AB-graphite dispersed well in the solvent used and was used both as a co-curing agent and as a nanoscale additive to the epoxy resin. The physical properties of resulting epoxy/AB-graphite composites were enhanced. This was because of the efficient load transfer through the covalent links between the AB-graphite and the epoxy resin.

## Experiment:

### 2.1 Materials

All the reagents and solvents used were purchased from Aldrich Chemicals Inc. and used as received, unless otherwise specified. Graphite (Aldrich Cat. No. 7782-42-5, type = powder, particle size < 45 µm, purity = 99.99+%) was also obtained from Aldrich Chemicals Inc. The epoxy resin used as the matrix material was diglycidyl ether of bisphenol A (DGEBA), supplied by the Kukdo Chemical Co. The curing agent 4,4'-diaminodiphenylmethane (MDA, purity ≥ 97%) was obtained from Alfa Aesar, USA.

### 2.2 Instrumentation

Fourier-transform infrared (FT-IR) spectra were recorded using a Bruker Fourier-transform spectrophotometer (Model spectrum 100). Elemental analysis was performed using a Thermo Scientific Flash 2000 analyzer. The field emission scanning electron microscope (FE-SEM) used in this work was a NanoSem 230 (FEI, USA). High-resolution transmission electron microscopy (HR-TEM) was performed using a JEM-2100F (JEOL, Japan). Epoxy/AB-graphite composite films were microtomed to a thickness of 50–70 nm at room temperature using a Reichert-Jung Ultracut microtome. The samples were mounted on 200-mesh copper grids.

Thermogravimetric analysis (TGA) was conducted in both air and nitrogen atmospheres employing a heating rate of 10 °C/min using a Q200 (TA Inst., USA). Wide-angle X-ray diffraction (WAXD) powder patterns were recorded with a Rigaku RU-200 diffractometer using Ni-filtered Cu K $\alpha$  radiation (40 kV, 100 mA,  $\lambda$  = 0.15418 nm). Dynamic mechanical analysis (DMA) was conducted using a Q800 (TA Inst., USA) at a frequency of 1 Hz using a film tension clamp. The samples were heated from room temperature (RT) to 250 °C at a rate of 5 °C/min. The storage modulus and tangent delta ( $\delta$ ) were measured. The sample films were cut into rectangular shaped samples with a length, width, and thickness of 30.0, 6.0, and (0.3–0.4) mm, respectively. Mechanical tests were performed using an Instron 3344 (ITW Co., USA) employing a 100-N load cell with a crosshead speed of 10 mm/min. The dog-bone-shaped tensile samples were prepared according to the recommendations in the ASTM D638 standard (Type V). All samples were cut using a laser cutter. The length, width, and thickness of the sample working dimensions were 9.53, 3.18, and (0.3–0.5) mm, respectively.

### *2.3 Edge-functionalization of “pristine” graphite using 4-aminobenzoic acid*

A mixture of 4-aminobenzoic acid (2 g), graphite (2 g), PPA (83% assay, 80 g), and P<sub>2</sub>O<sub>5</sub> (20 g) was placed into a resin flask equipped with a high torque mechanical stirrer, a nitrogen inlet valve, and an outlet valve. The mixture was stirred under a dry nitrogen purge at 80 °C for a period of 1 h. The reaction mixture was then heated to 100 °C and stirred for 1 h. Then, the mixture was heated to 130 °C and maintained at that temperature for 72 h. At the end of reaction, the color of the mixture was dark brown, and water was added to the flask contents. The resulting precipitate was washed with water and collected using suction filtration. The product was Soxhlet-extracted twice with methanol and water overnight and finally freeze-dried for a period of 48 h to give 3.26 g of a black powder (yield = 86.9%). Anal. calc. for C<sub>18.42</sub>H<sub>6</sub>NO (based on 100% conversion): C = 86.0%; H = 2.4%; O = 6.2%; N = 5.4%. Found: C = 85.9%; H = 1.9%; O = 7.1%; N = 5.1%.

### *2.4 Representative procedure for the preparation of epoxy/AB-graphite composites with a 1.0 wt% AB-graphite loading*

A stock solution of AB-graphite (1.0 g) was dispersed in ethanol (1 L) under magnetic stirring with a brief ultrasonication (5 min) applied to accelerate the dispersion of the AB-graphite. The AB-graphite solution (0.1 g AB-graphite in 100 mL) was then mixed well with epoxy resin (9.9 g). Then, the ethanol was completely removed under reduced pressure (0.05 mmHg) at 50 °C. The MDA curing agent (27 wt% vs. epoxy resin) was added and homogeneously mixed at room temperature to form the curable epoxy resin mixture. The mixture was cured as follows. Any persistent voids were further removed under reduced pressure prior to casting. Then, the mixture was poured on a leveled plate in a convection oven and precured at 80 °C for a period of 2 h and postcured at 150 °C for a period of 2 h to produce a cured film with a diameter of approximately 10 cm.

**Results and Discussion:** Elemental analysis (EA) showed that the “pristine” graphite contained a significant amount of hydrogen (0.2 wt%) because of the

$\text{sp}^2\text{C}-\text{H}$  groups at the edges of the graphite (Table 1). The value observed implies that the ratio of  $\text{sp}^2\text{C}-\text{H}$  group to carbon atoms present was 1:45.8. The  $\text{sp}^2\text{C}-\text{H}$  groups are the sites where the electrophilic substitution reactions will occur. As shown in Fig. 1, the edges of “pristine” graphite could be selectively functionalized with 4-aminobenzoic acid by a “direct” Friedel–Crafts acylation reaction in a  $\text{PPA}/\text{P}_2\text{O}_5$  mixture to produce 4-aminobenzoyl-functionalized graphite (AB-graphite).<sup>36</sup> Interesting changes in color were observed during the reaction. The initial color was black because of the dispersed graphite, but the solution turned to dark brown at the end of the reaction because of the functionalization of the 4-aminobenzoyl groups, and therefore, the exfoliation of graphite into graphene and graphene-like platelets. As described in the Experimental section, the powder product was fully worked-up by Soxhlet extraction with water and methanol overnight to minimize any unexpected variables. The former treatment was applied to remove excess reaction media and the latter treatment was applied to remove any unreacted 4-aminobenzoic acid. Finally, the samples were freeze-dried for a period of 48 h to afford the 86.9% yield of the black powder product. From the EA data, the resulting AB-graphite showed a similar carbon content between the experimental and theoretical values (Table 1).

**Table 1.** Elemental analysis of “pristine” graphite and AB-graphite.

Sample	Elemental analysis	C (%)	H (%)	O (%)	N (%)
Pristine graphite	Calc.	100.0	0.0	0.0	0.0
	Found	98.2	0.2	BLD	0.0
AB-graphite	Calc.	86.0	2.4	6.2	5.4
	Found	85.9	1.9	7.1	5.1

\* BLD = below the limit of detection.

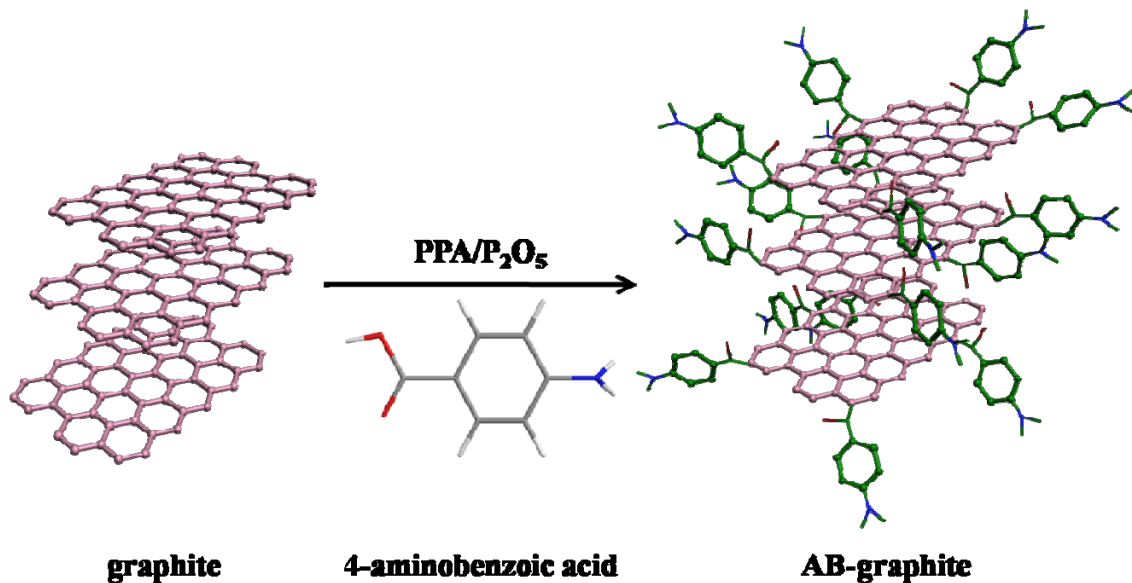


**Fig. 1** Edge-functionalization of “pristine” graphite using 4-aminobenzoic acid in a polyphosphoric acid/phosphorous pentoxide medium to produce 4-aminobenzoyl-functionalized graphite.

Fourier-transform infrared (FT-IR) spectroscopy is an important technique for studying functionalized carbon nanomaterials.<sup>34</sup> While “pristine” graphite shows a featureless spectrum (Fig. 2a), AB-graphite exhibits characteristic bands associated with primary amines ( $-\text{NH}_2$ ) occurring at  $1603\text{ cm}^{-1}$ , corresponding to the N–H bend vibrations (Fig. 2b). The C–N stretching band of an aromatic amine and an N–H out-of-plane bending occurred at  $1313$  and  $846\text{ cm}^{-1}$ , respectively. Furthermore, AB-graphite clearly showed an aromatic carbonyl ( $\text{C}=\text{O}$ ) peak centered at  $1651\text{ cm}^{-1}$ , which occurred at the covalent junctions between the 4-aminobenzoyl groups and graphite. These results provided further evidence that the 4-aminobenzoyl groups were covalently linked to the graphite.

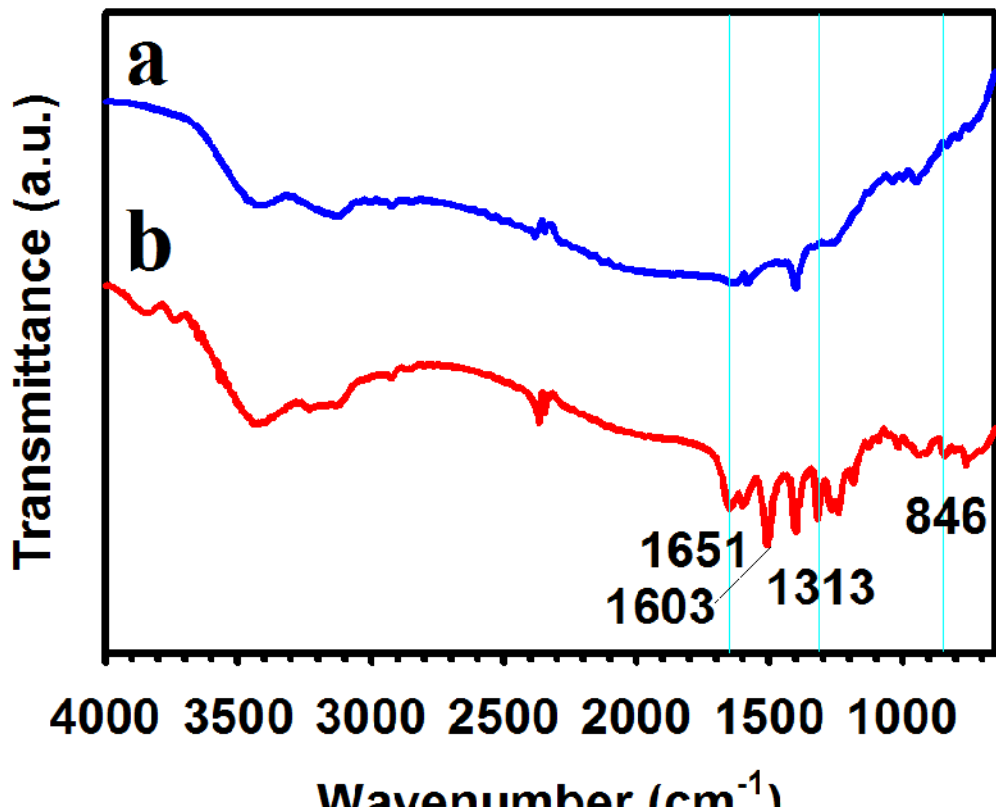


**Fig. 2** FT-IR (KBr pellet) spectra: (a) “pristine” graphite and (b) AB-graphite.

The degree of functionalization could be quantitatively estimated using thermogravimetric analysis (TGA). The “pristine” graphite showed almost no weight loss up to a temperature of 600 °C in air (Fig. 3a). On the other hand, AB-graphite showed a stepwise weight loss commencing at 488 °C in air (Fig. 3a). This early weight loss was attributed to the 4-aminobenzoyl (AB) moiety that was covalently attached to the edges of the graphite. The amount of weight loss at 750 °C was approximately 47 wt%. It is important to note that the subsequent degradation pattern of AB-graphite is practically congruent with that of “pristine” graphite. The residual amount at the temperature was 53 wt%. The portion should be thermooxidatively more stable graphite. The result strongly implies that a large amount of the AB moiety that was covalently attached to the AB-graphite. In nitrogen, “pristine” graphite was stable to 900 °C, while the AB-graphite showed a weight loss at 750 °C of approximately 23 wt% (Fig. 3b). The difference in weight loss between the air and nitrogen experiments was because a portion of the aromatic AB moieties was carbonized under inert conditions and became a thermally stable char.

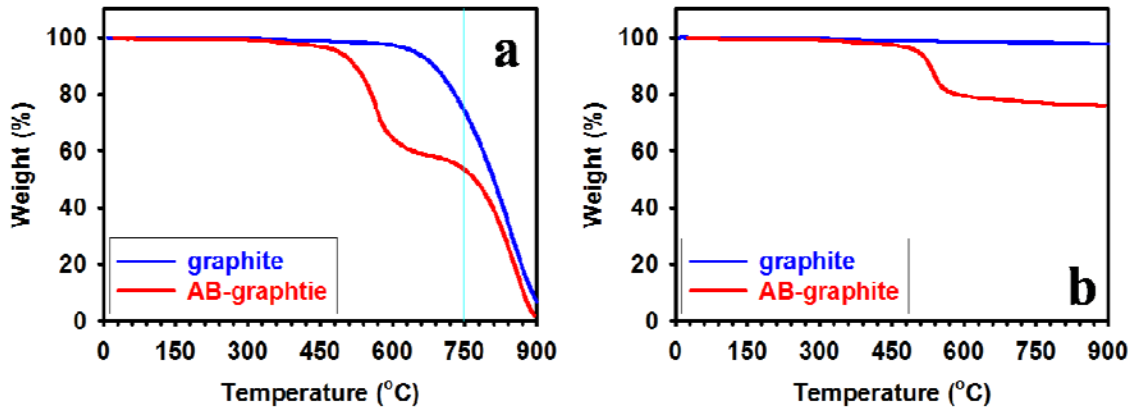


**Fig. 3** TGA curves of “pristine” graphite and AB-graphite using a heating rate of 10 °C/min: (a) in air and (b) in nitrogen.

Scanning electron microscopy images of “pristine” graphite showed that its surface was smooth and clean (Fig. 4a), while the surface of AB-graphite was rough and uneven because of the attachment of the AB moieties (Fig. 4b), which provides further evidence of the formation of AB-graphite from the reaction between 4-aminobenzoic acid and “pristine” graphite.

Transmission electron microscopy (TEM) was used to provide further visual confirmation of the results. The TEM samples were prepared as follows. AB-graphite was dispersed in ethanol, and then, a carbon grid containing holes was dipped into the solution, and the grid was dried in a vacuum oven. A typical TEM image of AB-graphite under low magnification is shown in Fig. 4c, showing exfoliated graphene and graphene-like platelets. An “edge-on” image under high magnification (Fig. 4d) and a selected area electron diffraction (SAED) pattern (inset, Fig. 4d) showed the presence of individual graphene with a high degree of crystallinity. Further TEM investigations indicated that a significant portion of the graphene consisted of individual and bilayer graphene (Figs. S1a–S1c in the Electronic Supplementary Information (ESI)), while a portion existed as graphene-like platelets with up to 15 graphene layers (Fig. S1d in the ESI).

The degree of exfoliation could be further estimated by using wide-angle x-ray diffraction (WAXD) patterns (Fig. S2 in ESI). The relative XRD peak intensity of AB-graphite to that of pristine graphite is approximately 33 % at 26.48° (d-spacing = 0.334 Å), which corresponds to van der Waals interlayer distance of graphene sheets, which remains constant after edge-selective functionalization. The intensity was approximately 67 % decreased due to the delamination of graphite into a few layers of AB-graphite (graphene-like platelets). The almost same peak location around 26.5° implies that AB-moiety was exclusively attached to the edges of graphite without the basal plane functionalization.

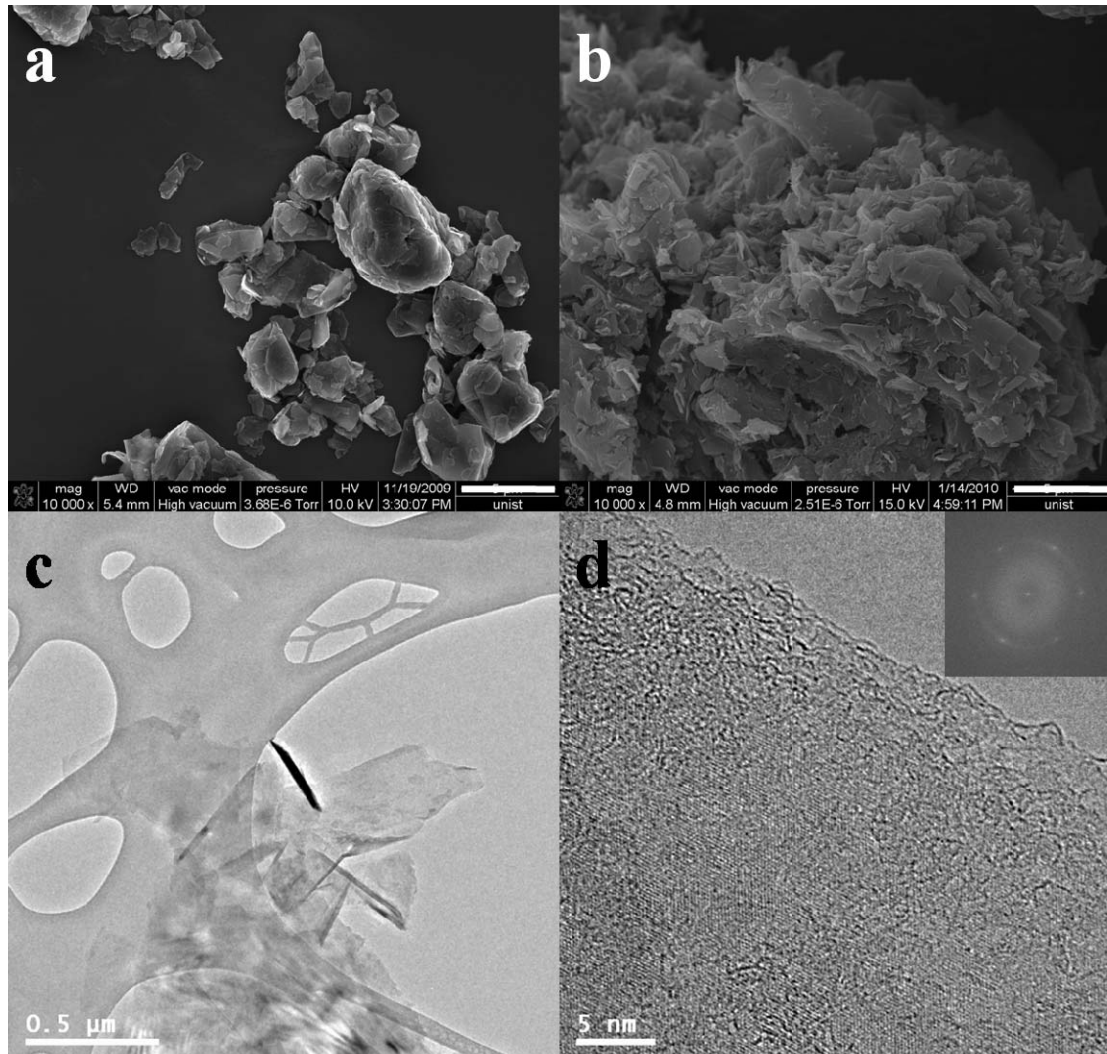


**Fig. 4** SEM images: (a) “pristine” graphite and (b) AB-graphite. The scale bars denote a distance of 5  $\mu\text{m}$ . TEM images of AB-graphite: (c) under low magnification and (d) under high magnification. The inset shows a selected area electron diffraction (SAED) pattern from the base area of (d).

The homogeneous dispersion of nanoscale additives into a supporting matrix and their interfacial interaction will have a significant effect on the resulting mechanical properties.<sup>37</sup> As described in the Experimental section, AB-graphite was used both as a co-curing agent and as a nanoscale additive to epoxy resin. Resin mixtures with different loadings of AB-graphite and MDA (27 wt% to DGEBA) were cast on a leveled plate and cured at elevated temperatures. The transmittance of the films decreased as the AB-graphite load increased (Fig. S3 in the ESI). The samples were tested using a dynamic mechanical analysis machine. The storage modulus ( $E'$ ) and  $\tan \delta$  value with respect to temperature was obtained to assess the role of the nanoscale additives under stress (Fig. 5). As is summarized in Table 2, the storage modulus of the composites at room temperature increased with increasing

AB-graphite load up to 2.0 wt% (Fig. 5a). The composite with an AB-graphite load of 2.0 wt% showed the highest storage modulus of  $E' = 2.5$  GPa, while the pure epoxy composite showed  $E' = 2.0$  GPa, an increase of 25%. The value saturated at loadings above 2 wt%. It should be due to the homogeneous dispersion was limited up to AB-graphite load 2 wt%. The composite with an AB-graphite loading of 4 wt% showed an initial storage modulus that was decreased slightly compared with the sample with a load of 2 wt%, but its storage modulus was the highest at temperatures above 100 °C.

Fig. 5b shows the temperature dependence of the  $\tan \delta$  values of the epoxy/AB-graphite composites. The  $\tan \delta$  value is defined as a loss factor, i.e., the ratio of the loss modulus to the storage modulus ( $E''/E'$ ), and is very sensitive to a structural transformation in a solid material. The maximum of the  $\tan \delta$  peak represents the glass transition temperature ( $T_g$ ) of a composite, and is shown in Table 2. The  $T_g$  value of the composites shifted to lower temperatures with increasing AB-graphite loading. This is possibly because increasing the graphite loading reduces the density of crosslinks in the epoxy resin,<sup>38</sup> and therefore, the mobility of the cured epoxy resin should be increased.

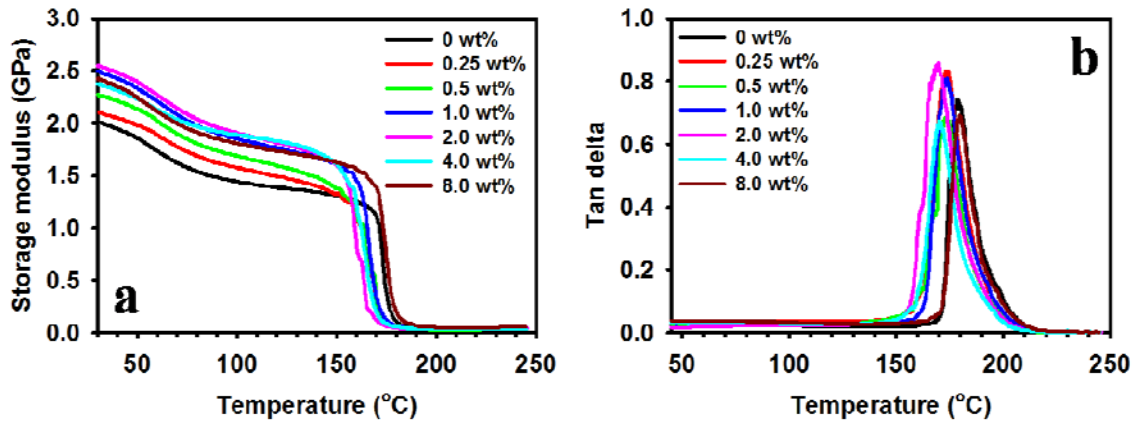


**Fig. 5** Dynamic mechanical analysis of epoxy/AB-graphite composites: (a) storage modulus ( $E'$ ) and (b)  $\tan \delta$ .

**Table 2.** Thermomechanical properties of AB-graphite/epoxy composites.

Loading (wt%)	Storage modulus (GPa)	$T_g$ (°C)
Pure epoxy	2.0	179
0.25	2.1	174
0.50	2.3	174
1.00	2.5	174
2.00	2.5	171
4.00	2.4	171
8.00	2.4	180

The tensile properties of filler-reinforced composites are significantly

influenced by the interactions between the filler and the supporting matrix.<sup>39</sup> The epoxy/AB-graphite composite films were prepared as dog-bone-shaped samples, based on the recommendations in the ASTM D638 standard (Type V) (Fig. S4 in the ESI). The dimensions of the samples were length = 64 mm, width = 9.5 mm, and thickness = approximately 0.5 mm (Fig. S4 in the ESI). The representative stress-strain curves of samples with different AB-graphite loading are shown in Fig. 6a. The average values with standard deviation are shown in Fig. 6b, and the results are summarized in Table 3. Compared with pure epoxy, both the tensile strength and the Young's modulus of the epoxy/AB-graphite composites were improved for all compositions studied. The average tensile strength at break for pure epoxy and epoxy/AB-graphite with a loading of 4 wt% were 61 MPa and 79 MPa, respectively; i.e., an increase of approximately 30%. In the case of the Young's modulus, the composite with an AB-graphite loading of 4 wt% showed the maximum average modulus of 983 MPa, an improvement of more than 40%. The remarkable improvement in the tensile strength and the Young's modulus is attributable to the covalent links formed between the AB-graphite and the epoxy matrix. Further increasing the AB-graphite loading above 4 wt% led to a decrease in both the tensile strength and the Young's modulus. It is assumed that the degree of AB-graphite dispersion was low, and thus, some aggregates may have acted as defect centers. As a result, it was concluded that an AB-graphite loading of approximately 4.0 wt% is the critical concentration for the maximum enhancement in properties. These results imply that AB-graphite can be efficiently dispersed in an epoxy matrix when the AB-graphite loading is < 4 wt%. On increasing the AB-graphite loading, the restacking of the AB-graphite leads to the formation of aggregates, saturating the reinforcing efficiency of the composites.

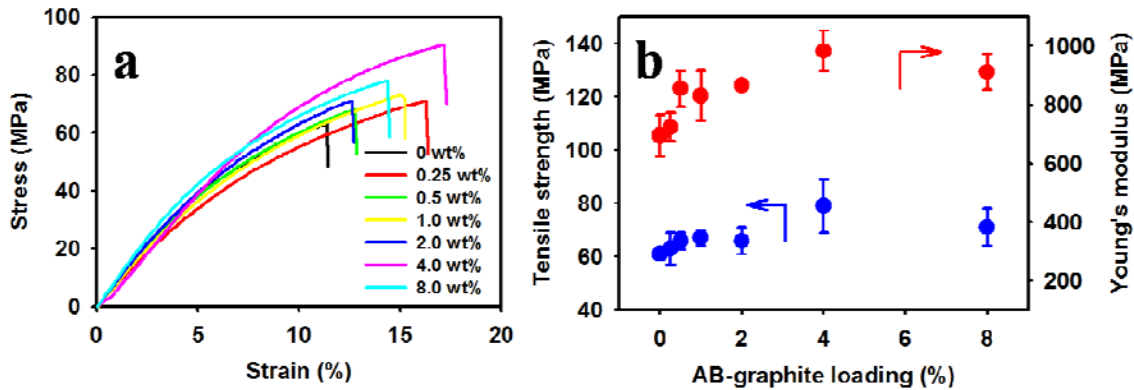


**Fig. 6** (a) Stress–strain curves of epoxy and epoxy/AB-graphite composite films. (b) The average tensile strength and Young's modulus of epoxy and epoxy/AB-graphite composites.

**Table 3.** Tensile properties of epoxy/AB-graphite composites.

Load (wt%)	Tensile strength (MPa) <sup>a</sup>	Young's modulus (MPa) <sup>a</sup>
Pure epoxy	$61 \pm 2$	$695 \pm 70$
0.25	$63 \pm 6$	$723 \pm 50$
0.50	$66 \pm 3$	$855 \pm 60$
1.00	$67 \pm 3$	$831 \pm 85$
2.00	$66 \pm 5$	$867 \pm 20$
4.00	$79 \pm 10$	$983 \pm 70$
8.00	$71 \pm 7$	$912 \pm 60$

a. The value shown is the average of seven samples tested.

The degree of dispersion of a nanoscale additive in a supporting matrix directly correlates with the mechanical, electrical, barrier, and many other properties of a composite.<sup>29</sup> Thus, the origin of the improved mechanical properties can be anticipated visually from microscopic observation. The SEM images were obtained from the fracture surface of epoxy films and epoxy/AB-graphite composite films with an AB-graphite loading of 2.0 wt%. The surface of pure epoxy films shows a smooth fracture surface, indicating that the material is brittle without any ductility (Fig. 7a and 7b). On the other hand, the surface of the epoxy/AB-graphite films is rough, and the AB-graphite is uniformly distributed in the epoxy matrix (Fig. 7c and 7d). Because of the high degree of dispersion of AB-graphite in the cured epoxy resin, it was difficult to observe the formation of any aggregates. The AB-graphite was embedded well into and tightly bound to the matrix. Because covalent links between the amine groups of the AB-graphite had formed, a boundary between the AB-graphite and the epoxy matrix could not be discerned. These covalent links provided a strong interfacial adhesion between the AB-graphite and the epoxy resin, resulting in an efficient transfer of the load.

For the comparison purpose, controlled experiment was carried out. Epoxy/graphite composite with 2 wt% “pristine” graphite load was prepared from the

very similar procedure for the epoxy/AB-graphite system. The SEM images obtained from the fractured surface of epoxy/graphite composite film is also presented (Fig. S5a-c in the ESI). It is obvious that the interface between graphite and cured epoxy matrix is clearly discernable and not well bonded (Fig. S5c, arrow in the ESI). On the other hand, it is difficult to discern the interface between AB-graphite and cured epoxy resin (Fig. S5d-f in the ESI), indicating that they are bonded well. The result implicates that the covalent linkages between AB-graphite and epoxy resin were formed to show enhanced physical properties.

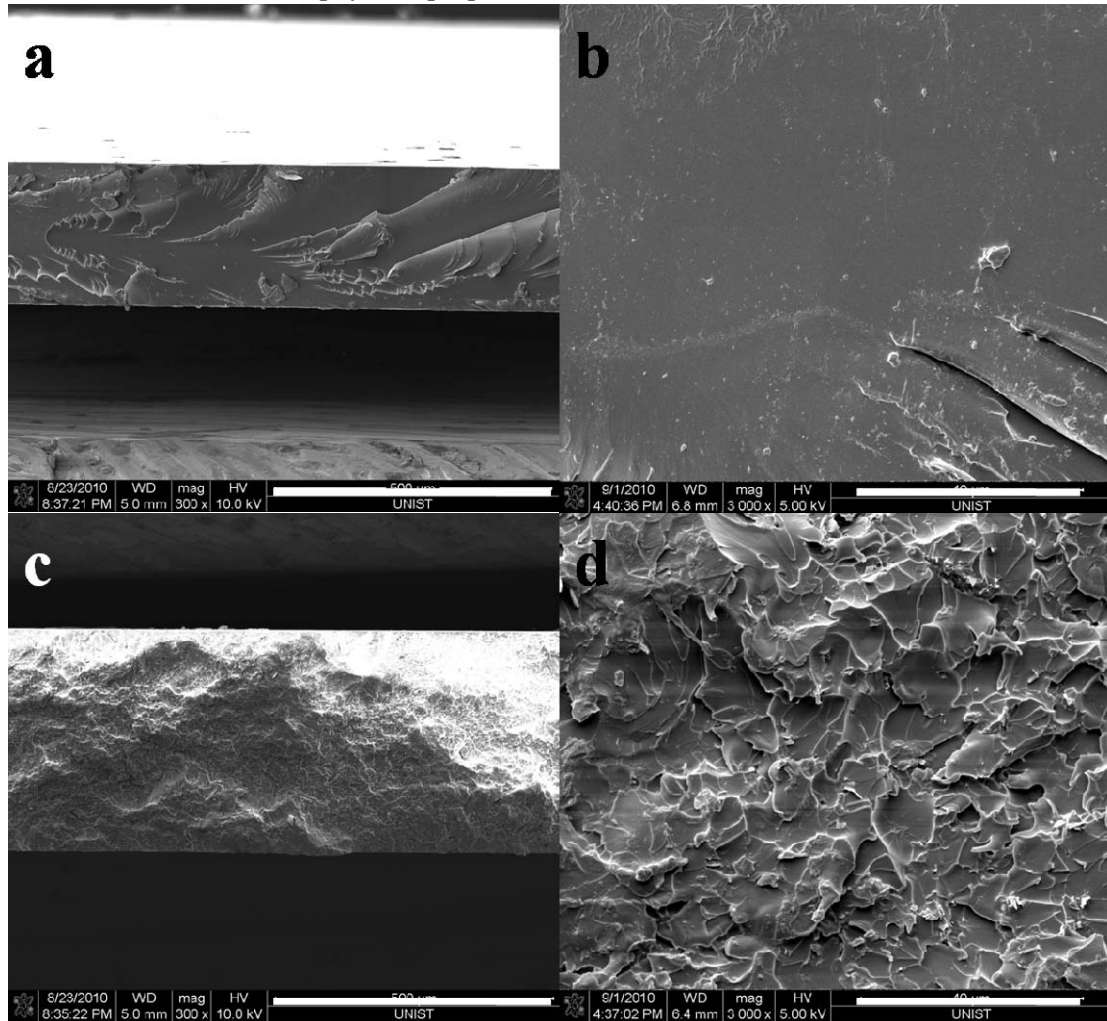


**Fig. 7** SEM images obtained from fracture surfaces of films after tensile tests: (a) pure epoxy; (b) a magnified image of 7(a). Scale bars are 500 and 40  $\mu$ m, respectively; (c) an epoxy/AB-graphite composite with an AB-graphite loading of 2 wt%; and (d) a magnified image of 7(c). Scale bars are 500 and 40  $\mu$ m, respectively.

Furthermore, the epoxy/AB-graphite composite film with an AB-graphite loading of 2 wt% was microtomed and placed on a carbon-coated grid. The TEM images showed that the AB-graphite existed in the form of a few layers composed of graphene platelets (Fig. 8a). Because of their flexibility, the thin graphene platelets

appeared to be crumpled and wrinkled in the cured epoxy matrix. The graphene platelets were distorted into ribbon shapes and scrolled into a helical ribbon (Fig. 8b, denoted by the arrow).

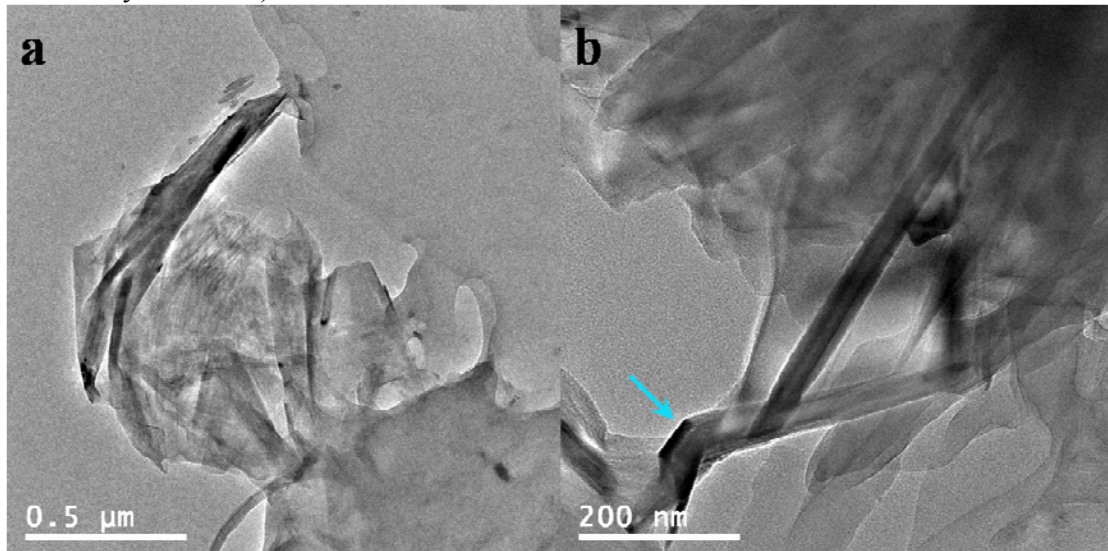


**Fig. 8** TEM images obtained from an epoxy/AB-graphite sample containing 2 wt% of AB-graphite after microtoming of the sample: (a) under low magnification and (b) at higher magnification.

In summary, Using a newly developed method for edge-selective functionalization in a PPA/P<sub>2</sub>O<sub>5</sub> mixture, graphite was functionalized with 4-aminobenzoic acid to produce 4-aminobenzoyl-functionalized graphite (AB-graphite) that could be used as a co-curing agent and as a nanoscale additive to an epoxy resin. Based on our characterization, the resulting AB-graphite was well functionalized with 4-aminobenzoyl groups. The AB-graphite was dispersed in many polar solvents, including ethanol, which was selected as the medium for the preparation of epoxy/AB-graphite composites. The mechanical properties of the composite films were significantly improved compared with pure epoxy films. Our results suggest that AB-graphite plays the role of a co-curing agent and as a nanoscale additive.

#### List of Publications

1. Choi, E.-K.; Jeon, I.-Y.; Shin, Y. R.; Baek, J.-B. "Strain-induced delamination of edge-grafted graphite" *Chemical Communications* **2012**, accepted.
2. Chang, D. W.; Bae, S.-Y.; Dai, L.; Baek, J.-B. "Efficient energy transfer between amphiphilic dendrimers with oligo(p-phenylenevinylene) core branches and oligo(ethylene oxide) termini in micelles" *Journal of Polymer Science, Part A: Polymer Chemistry* **2012**, accepted.
3. Sohn, G.-J.; Choi, H.-J.; Jeon, I.-Y.; Chang, D. W.; Dai, L.; Baek, J.-B. "Water-dispersible, sulfonated hyperbranched poly(ether-ketone) grafted multi-walled carbon nanotubes as oxygen reduction catalysts" *ACS Nano* **2012**, 6, 6345-6355.
4. Choi, H.-J.; Jung, S.-M.; Seo, J.-M.; Chang, D. W.; Dai, L.; Baek, J.-B.

“Graphene for Energy Conversion and Storage” *Nano Energy* **2012**, 1, 534-551.-**Invited Review Article**.

5. Kumar, N. A.; Choi, H.-J.; Bund, A.; Baek, J.-B.; Jeong, Y. T. “Electrochemical supercapacitors based on a novel graphene/conjugated polymer composite system” *Journal of Materials Chemistry* **2012**, 22, 12268-12274.
6. Jeon, I.-Y.; Shin, Y.-R.; Sohn, G.-J.; Choi, H.-J.; Bae, S.-Y.; Mahmood, J.; Jung, S.-M.; Seo, J.-M.; Kim, M.-J.; Chang, D.-W.; Dai, L.; Baek, J.-B. “Edge-carboxylated graphene nanosheets via ball milling” *Proceedings of the National Academy of Sciences, USA* **2012**, 109, 5588-5593.-**Highlighted in Chosun.com, KBS World, and Science Daily and more than 100 times global News Hits**.
7. Wang, S.; Zhang, L.; Xia, Z.; Roy, A.; Chang, D. W.; Baek, J.-B.; Dai, L. “BCN graphene as efficient metal-free electrocatalyst for oxygen reduction reaction” *Angewandte Chemie International Edition* **2012**, 124, 4209-4212.-**Selected as Hot Paper**.
8. Kumar, N. A.; Choi, H.-J.; Chang, D. W.; Dai, L.; Baek, J.-B. “Covalent grafting of conducting polyaniline/graphene nanocomposite and its use as efficient electrochemical supercapacitors” *ACS Nano* **2012**, 6, 1715-1723.-**Top Twenty Most Read Articles during March, 2012, Highlighted in Graphene Times.com**.
9. Dai, L.; Chang, D. W.; Baek, J.-B.; Lu, W. “Carbon Nanomaterials for Advanced Energy Conversion and Storage” *Small* **2012**, 8, 1130-1166.-**Selected as Inside Cover**.
10. Choi, H.-J.; Kang, J.-Y.; Jeon, I.-Y.; Eo, S.-M.; Baek, J.-B. “Immobilization of Platinum Nanoparticles on *ortho*-Diaminobenzoyl-Functionalized Multi-Walled Carbon Nanotube and Its Electrocatalytic Activity” *Journal of Nanoparticle Research* **2012**, 14, 704.
11. Shin, Y.-R.; Jeon, I.-Y.; Baek, J.-B. “Stability of multi-walled carbon nanotubes in different acidic media” *Carbon* **2012**, 50, 1645-1476.
12. Choi, H.-J.; Jeon, I.-Y.; Kang, S.-W.; Baek, J.-B. “Electrochemical activity of PANi/PANi-g-MWCNT mixture by simple suspension polymerization” *Electrochimica Acta* **2011**, 56, 10023-10031.
13. Jeon, I.-Y.; Yu, D.; Bae, S.-Y.; Choi, H.-J.; Chang, D. W.; Dai, L.; Baek, J.-B. “Formation of Large-Area Nitrogen-Doped Graphene Film Prepared from Simple Solution Casting of Edge-Selectively Functionalized Graphite and Its Electrocatalytic Activity” *Chemistry of Materials* **2011**, 23, 3987-3992.-**(Top Twenty Most Read Articles during September, 2011, Highlighted in Graphene Times.com)**.
14. Wang, S.; Yu, D.; Dai, L.; Chang, D. W.; Baek, J.-B. “Polyelectrolyte-functionalized graphene as metal-free electrocatalyst for oxygen reduction” *ACS Nano* **2011**, 5(8), 6202-6209.-**Top Twenty Most Read Articles during September, 2011, Highlighted in Graphene Times.com**
15. Bae, S.-Y.; Jeon, I.-Y.; Yang, J.; Park, N.; Shin, H. S.; Park, S. J.; Ruoff, R. S.; Dai, L.; Baek, J.-B. “Large-area graphene films by simple solution casting of edge-selectively functionalized graphite” *ACS Nano* **2011**, 5(6), 4974-4980.-**Top Twenty Most Read Articles during June, 2011, Highlighted**

**in NANOWERK, Highlighted in Graphene Times.com, Highlighted in Graphene Times.com, Highlighted in NATURE Asia Materials.**

16. Jeon, I.-Y.; Choi, H.-J.; Bae, S.-Y.; Chang, D.-W.; Baek, J.-B. "Wedging graphite into graphene and graphene-like platelets by dendritic macromolecules" *Journal of Materials Chemistry* **2011**, 21(21), 7820-7826.
17. Jeon, I.-Y.; Tan, L.-S.; Baek, J.-B. "Nanocomposite Prepared from *in-Situ* Grafting of Polypyrrole to Aminobenzoyl-Functionalized Multi-Walled Carbon Nanotube and Its Electrochemical Properties" *Journal of Polymer Science, Part A: Polymer Chemistry* **2011**, 49, 2529-2537.
18. Kim, K.-S.; Jeon, I.-Y.; Ahn, S.-N.; Kwon, Y.-D.; Baek, J.-B. "Edge-functionalized graphene-like platelets as a co-curing agents and nanoscale additive to epoxy resin" *Journal of Materials Chemistry* **2011**, 21, 7337-7342.
19. Kumar, N. A.; Jeon, I.-Y.; Sohn, G.-J.; Jain, R.; Kumar, S.; Baek, J.-B. "Highly conducting and flexible few-walled carbon nanotubes thin film" *ACS Nano* **2011**, 5(3), 2324-2331.
20. Choi, H.-J.; Jeon, I.-Y.; Chang, D. W.; Yu, D.; Dai, L.; Tan, L.-S.; Baek, J.-B. "Preparation and electrocatalytic activity of gold nanoparticles immobilized onto the surface of mercaptobenzoyl-functionalized multi-walled carbon nanotubes" *Journal of Physical Chemistry C* **2011**, 115, 1746-1751.